Fullerene negative ions: Formation and catalysis

Z. Felfli, K. Suggs, N. Nicholas, and A. Z. Msezane[#]
Clark Atlanta University, Department of Physics and CTSPS, Atlanta, Georgia 30314

Abstract

We first explore negative-ion formation in fullerenes C_{44}, C_{60}, C_{70}, C_{98}, C_{112}, C_{120}, C_{132} and C_{136} through low-energy electron elastic scattering total cross sections calculations using our Regge-pole methodology. Water oxidation to peroxide and water synthesis from H_2 and O_2 are then investigated using the anionic catalysts C_{44}^- to C_{136}^-. The fundamental mechanism underlying negative-ion catalysis involves hydrogen bond strength-weakening in the transition state. DFT transition state calculations found C_{60}^- numerically stable for both water and peroxide synthesis, C_{100}^- increases the energy barrier the most and C_{136}^- the most effective catalyst in both water synthesis and oxidation to H_2O_2.

[#]Corresponding author
amsezane@cau.edu

PACs.: 34.80.Bm Electron elastic scattering

Keywords: Fullerene anions; electron cross sections; polarization interaction; water oxidation; anionic catalysis

1. Introduction

To celebrate the International Year of the Periodic Table, the Royal Society of Chemistry published the themed collection '**Single Atoms as Active Catalysts**' [1]. This has motivated the present investigation. We first investigate the formation of negative ions in the fullerene molecules C_{44}, C_{60}, C_{70}, C_{98}, C_{112}, C_{120}, C_{132} and C_{136} through low-energy electron elastic scattering total cross sections (TCSs) calculations. Our robust Regge-pole methodology is used for the calculations. The formed anionic fullerenes C_{44}^- to C_{136}^- during the collisions are then used to investigate the catalysis of water oxidation to peroxide and water synthesis from H_2 and O_2.

Within the context of muon catalyzed nuclear fusion, our research group proposed and investigated theoretically the fundamental mechanism underlying atomic negative-ion catalysis [2, 3]. Negative ion catalysis involves anionic molecular complex formation in the transition state, with the atomic negative ion weakening/breaking the hydrogen bond strength. The mechanism of negative-ion catalysis has been demonstrated in the oxidation of H_2O to H_2O_2 catalyzed using the Au^- and Pd^- anions to understand the experiments of Hutchings and collaborators [4-6], in the catalysis of light, intermediate and heavy water to the corresponding peroxides [7] and in the oxidation of methane to methanol without the CO_2 emission [8] to name a few. Recently, the experiment [6] used the less expensive atomic Sn catalyst for possible water purification in the developing world. Consequently, here we explore the effectiveness of the fullerene negative ions C_{44}^- to C_{136}^- in the catalysis of water oxidation to peroxide and water synthesis from H_2 and O_2 in search of less expensive catalysts. The focus is particularly on the lager fullerene molecules greater than C_{70}.

The importance of fullerene molecules in fullerene negative ion catalysis, fullerenes for organic solar-cells, sensor technology, drug delivery, fullerene catalytic efficiency in fundamental hydrogenation, etc. has motivated us to study the variation of the electron affinity (EA) with the fullerene size from C_{44} to

C_{136} and contrasted the EAs with that of the standard C_{60}. Manifesting the existence of long-lived negative ion formation, reliable atomic and molecular affinities are crucial for understanding the vast number of chemical reactions involving negative ions [9]. In the formation of fullerene negative ions, it has been demonstrated for the first time that the ground state anionic binding energies (BEs) extracted from our Regge-pole calculated TCSs for the C_{20} through C_{92} fullerenes matched excellently the measured EAs [10-17]. This provides a novel and general approach to the determination of reliable EAs for complex heavy systems. Indeed, the EAs provide a stringent test of theoretical calculations when their results are compared with those from reliable measurements. And the Regge-pole methodology requires no assistance whatsoever from either experiment or other theory for the remarkable feat. The results [18, 19] provided great credence to the power and ability of the Regge-pole methodology to extract reliable EAs of the fullerene molecules from the calculated ground states electron elastic TCSs. It is noted here that obtaining unambiguous and reliable fullerene EAs is a challenging task for existing theoretical methods. Generally, the Regge-pole calculated low-energy electron elastic TCSs for fullerene molecules are characterized by ground, long-lived polarization-induced metastable and excited negative ion formation.

Except for the C_{60} fullerene theoretical and/or experimental low-energy electron elastic scattering TCSs for fullerenes are generally sparse. For C_{60} low-energy electron scattering cross sections have been investigated theoretically [20-27]. Very recently, angle-differential electron elastic scattering from C_{60} has been studied [28]. The investigations of Wigner Time Delay in electron - C_{60} elastic scattering [29] using potential models defined by the fullerene EA and its radius will certainly benefit from this study. Experimentally, low-energy electron elastic scattering differential cross sections for C_{60} were measured [30]. Gas phase fullerenes C_{76} and C_{78} [31] and gas phase C_{60} and C_{70} [32] have been studied using low-energy electron scattering. In the latter study, several resonant states were identified including the determination of the lifetimes of the formed negative ions. Thermal rate coefficients and cross sections for electron attachment to C_{60} have been studied [33] including their low energy temperature dependence in a crossed electron beam–molecular beam experiment [34],

The low-energy electron elastic collision TCSs of the fullerene molecules obtained in this paper as well as those of the already studied fullerenes [18, 19, 35, 36] and the actinide [37] and the lanthanide [38, 39] atoms should contribute to a better understanding of the role of the individual atoms/fullerenes in ongoing studies involving endohedral systems [40-46]. Also expected to benefit from this study will be the exploration of the $M@C_{60}$ (M = Ti, Zr, U) fullerene hybrids that have demonstrated catalytic efficiency in fundamental hydrogenation [47].

2. Method of Calculation

In [48] it was confirmed that Regge poles formed during low-energy electron elastic scattering become stable bound states. Here we adopt the Regge-pole methodology, also known as the complex angular momentum (CAM) method for the calculation of the electron scattering TCSs. Regge poles, singularities of the S-matrix, rigorously define resonances [49, 50]. Being generalized bound states, they can be used to calculate reliably the anionic BEs of the ground, metastable and excited states of complex heavy systems through the TCSs calculations. The Mulholland formula [51] is used here to calculate the near-threshold electron–fullerene collision TCS resulting in negative ion formation as resonances. In the form below, the TCS fully embeds the essential electron-electron correlation effects [52, 53] (atomic units are used throughout):

$$\sigma_{tot}(E) = 4\pi k^{-2}\int_0^{\infty} \mathrm{Re}[1-S(\lambda)]\lambda d\lambda$$
$$-8\pi^2 k^{-2}\sum_n \mathrm{Im}\frac{\lambda_n \rho_n}{1+\exp(-2\pi i\lambda_n)} + I(E) \qquad (1)$$

In Eq. (1) S(λ) and λ are respectively the S-matrix and the CAM, $k=\sqrt{2mE}$, m being the mass and E the impact energy, ρ_n is the residue of the S-matrix at the n^{th} pole, λ_n and $I(E)$ contains the contributions from the integrals along the imaginary λ-axis; its contribution has been demonstrated to be negligible [54].

As in [26] the complicated details of the electronic structure of the fullerene itself are not considered here. The incident electron is assumed to interact with the complex atom/fullerene through the Thomas-Fermi type potential, known as the ABF [55] which accounts for the vital core-polarization interaction

$$U(r)=-\frac{Z}{r(1+\alpha Z^{1/3}r)(1+\beta Z^{2/3}r^2)} \qquad (2)$$

In Eq. (2) Z is the nuclear charge, α and β are variation parameters. This potential has the appropriate asymptotic behavior, *viz.* $\sim -1/(\alpha\beta r^4)$ and accounts properly for the polarization interaction at low energies. This potential, extensively studied [56], has five turning points and four poles connected by four cuts in the complex plane. The presence of the powers of Z as coefficients of r and r^2 in Eq. (2) ensures that spherical and non-spherical atoms/fullerenes are correctly treated. The effective potential $V(r)=U(r)+\lambda(\lambda+1)/2r^2$ is considered here as a continuous function of the variables r and complex λ. The details of the numerical evaluations of the TCSs have been described in [53] and further details of the calculations may be found in [57].

In the calculations, the optimal value of α was determined to be 0.2. When the TCS as a function of β has a dramatically sharp resonance [54], corresponding to the formation of a stable negative ion, this resonance is longest lived for a given value of the energy, which corresponds to the EA of the system (for ground state collisions) or the BE of the metastable/excited anion. Also calculated in the CAM methods are the Regge Trajectories, viz. *Im* λ_n(E) versus *Re* λ_n(E); they have been used to demonstrate that at low energy relativistic and non-relativistic calculations yield the same results [58].

3. Results.

In Section 3.1 we first present the variation with the electron impact energy E of the Regge-pole calculated electron elastic scattering TCSs for the fullerene molecules C_{44} to C_{136}. Section 3.2 demonstrates the utility of the fullerene molecular anions in the catalysis of water oxidation to peroxide and water synthesis from H_2 and O_2 using the anionic fullerene catalysts C_{44}^- to C_{136}^-..

3.1 Fullerene electron scattering total cross sections

In fullerene negative ion formation, it has been demonstrated for the first time that the ground state anionic BEs extracted from our Regge-pole calculated electron elastic scattering TCSs for the C_{20} through C_{92} fullerenes matched excellently the measured EAs of these fullerenes [18, 19]. This provides a novel and general approach to the determination of unambiguous and reliable EAs for complex heavy systems. The Regge-pole methodology requires no assistance whatsoever from either experiment or other theory to achieve the remarkable feat.

Figures 1 and 2 present the elastic TCSs for the fullerene molecules C_{44} through C_{136} and Table 1 summarizes the essential data. Indeed, the Regge-pole calculated low-energy electron elastic TCSs for the fullerene molecules considered here are found to be characterized generally by ground, polarization-induced metastable and excited negative ion formation. For ground state collisions the resultant anionic BEs yield the theoretically challenging to calculate EAs and demonstrate their wide variation from fullerene to fullerene. The results here are consistent with the observation that low-energy electron-fullerene interactions are generally characterized by rich resonance structures [32, 59-61] and that the experimentally detected fullerene isomers correspond to the metastable states [62]. They also

support the conclusion that the EAs of fullerene molecules are relatively large [63]. This should satisfy part of the requirement to increase fullerene acceptor resistance to degradation by the photo-oxidation mechanism as well as improve the understanding of the degradation mechanism in organic solar cells [64]. The determined EAs here could also be employed to construct the widely used simple model potentials for the fullerene shells, including endohedral fullerenes [65]. The resonance-rich structures of the fullerene TCSs and their large EAs explain the tendency of fullerenes to form compounds with electron-donor anions and their vast applications as well. These TCSs require careful delineation and identification of the attendant resonance structures for reliable interpretation as well as extraction of the EAs.

For a better appreciation of the physics underlying the resonance-rich TCSs for the various fullerenes presented in the Figs. 1 and 2, we first discuss briefly the TCSs for the C_{44} fullerene. With less structure, the TCSs were first calculated in [18]; here they have been recalculated to expose more resonances. It is noted that generally the internal region of zero potential provided by the hollow cage structure of the fullerenes is conducive to metastable anionic formation during the collisions. This is clearly manifested through the appearance of additional resonances in the TCSs as the fullerene size increases from C_{44} through C_{136}. Also, this explains the existence of the two series of resonances, the first is associated with the ground state TCS while the second belongs to the highest excited state TCS (green curve).

Focusing specifically on the C_{44} TCSs, Fig. 1(a), the red, blue, pink, brown and green curves represent respectively the TCSs of the ground; the first & the second metastable and the two excited states. The fundamental physics underlying these curves can be readily understood if we focus on each color-coded TCS. For the analysis we select the ground state TCS curve, the red curve. Near threshold the TCS exhibits the characteristic shape resonance (SR), broad maximum. As the electron energy is increased, the fullerene becomes polarized and reaches maximum polarization manifested through the appearance of the first R-T minimum at about 1.01 eV, indicative that the polarization interaction has been accounted for adequately in the calculation [66]. With further increase in the electron impact energy, the electron becomes trapped by the centrifugal potential, demonstrated by the appearance of the SR at 1.41 eV. As the electron leaks out of the centrifugal potential, the C_{44} shell, due to its strong polarizability, becomes significantly polarized leading to the generation of the second deep R-T minimum in the TCS at 3.13 eV. At the absolute minimum the long-lived ground state of the C_{44}^- anion is formed with the BE of 3.15 eV. At the R-T minimum the electron spends many angular rotations about the C_{44} as it decays; the angular life is determined by $1/[\mathrm{Im}\ \lambda_n(E)] \rightarrow \infty$, since for the ground state resonance $\mathrm{Im}\ \lambda_n(E) \rightarrow 0$, see Eq. (1). Notably, at the R-T minimum new molecules can be created from fermions.

The analysis is also applicable to the other fullerene TCSs presented in Fig. 1 as well as in Fig. 2. The extracted BEs of the negative ions formed during the collisions are summarized in Table 1 where they are compared with available EAs. Indeed, for the ground state collisions the extracted from the TCSs anionic BEs correspond to the EAs of the fullerenes. The Regge-pole calculated TCSs for the C_{60} fullerene presented in Fig. 1(b) is taken from [39]. The TCSs, typical of those calculated in this paper, are found to be characterized generally by dramatically sharp resonances manifesting ground, metastable and excited anionic formation during the collisions, Ramsauer-Townsend (R-T) minima and shape resonances. Indeed, the ground state TCS (red curve) yields the anionic BE, located at its absolute R-T minimum; it has been identified with the C_{60} EA [19]. Viewed as presented in the Fig. 1(b) the C_{60} TCSs appear complicated as well. However, they are readily understood and interpreted as was done in [19] and [39]. This ground state TCS is clearly shown alone in Fig. 1 of [19] and the underlying physics is also presented there.

Figures 1(b) to 2 demonstrate the variation of the electron TCSs with E for the C_{60}, C_{70}, C_{98}, C_{112}, C_{120}, C_{132} and C_{136} fullerene molecules. Clearly, these TCSs are characterized as in the C_{44} case by ground, metastable and excited anionic formation, R-T minima and shape resonances. The extracted anionic BEs

Preprints (www.preprints.org) | NOT PEER-REVIEWED | Posted: 28 February 2020 doi:10.20944/preprints202002.0420.v1

Peer-reviewed version available at Int. J. Mol. Sci. 2020, 21, 3159; doi:10.3390/ijms21093159

from the ground states TCSs correspond to the EAs of the fullerene molecules. These BEs, presented in Table 1 demonstrate their wide variation from fullerene to fullerene. The various dramatically sharp resonances in the TCSs represent negative ion formation in the ground, metastable and excited states.

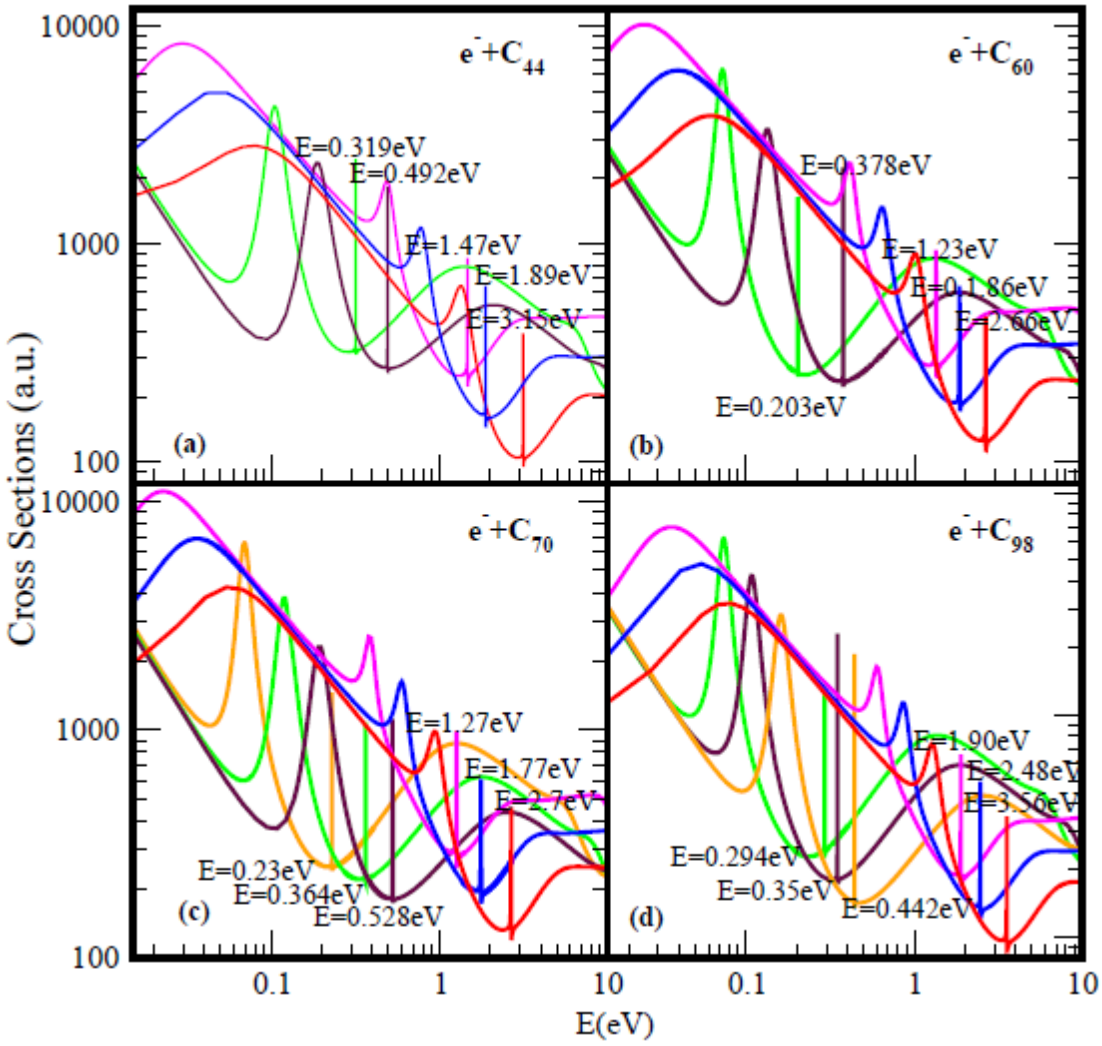

Figure 1: Total cross sections (a.u.) for (a) C_{44}, (b) C_{60}, (c) C_{70} and (d) C_{98}. The red, blue and pink curves represent TCSs for the ground and induced metastable states (first and second), respectively. The green and brown curves in (a) and (b) denote the TCSs for the first and the second excited states, respectively. For C_{70} and C_{98} the orange, green and brown curves represent the excited states TCSs. The dramatically sharp resonances correspond to the fullerene anions formed during the collisions**.**

Preprints (www.preprints.org) | NOT PEER-REVIEWED | Posted: 28 February 2020 doi:10.20944/preprints202002.0420.v1

Peer-reviewed version available at Int. J. Mol. Sci. 2020, 21, 3159; doi:10.3390/ijms21093159

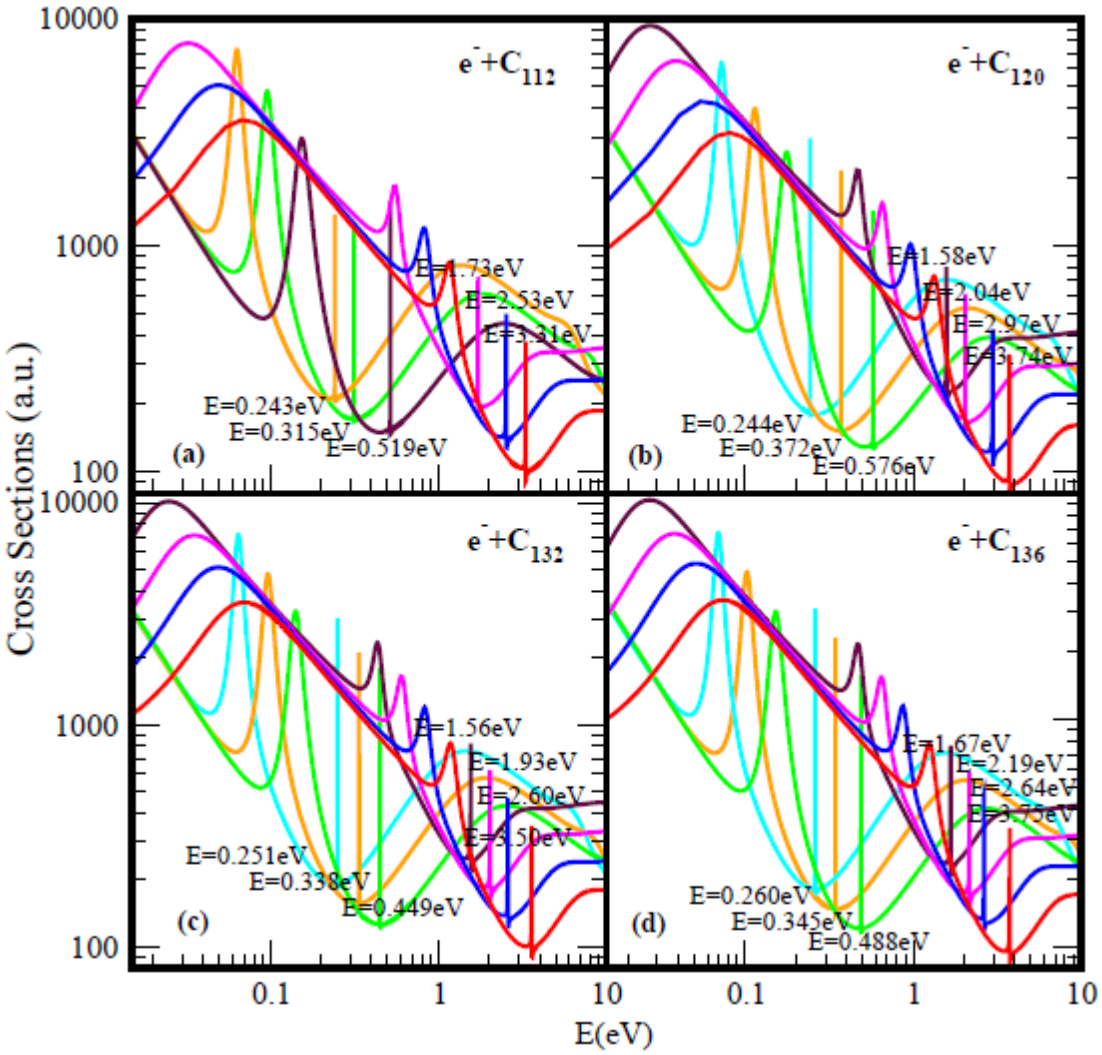

Figure 2: Total cross sections (a.u.) for (a) C_{112}, (b) C_{120}, (c) C_{132} and (d) C_{136}. The red, blue, pink and brown (no brown curve for C_{112}) curves represent TCSs for the ground and induced metastable states (first, second and third), respectively. For C_{112} (orange, green and brown), while for C_{120}, C_{132} and C_{136} (light blue, orange and green) curves correspond to the excited TCSs. The dramatically sharp resonances correspond to the anions formed during the collisions.

3.2 Fullerene transition state barriers

The utility of the fullerene negative ions has been demonstrated in the catalysis of water oxidation to peroxide and water synthesis from H_2 and O_2 using the anionic fullerene catalysts C_{44}^- to C_{136}^-. Figures 3 and 4 demonstrate the Density Functional Theory (DFT) calculated transition states. DFT and dispersion corrected DFT approaches have been employed for the transition state evaluations. Geometry optimization of the structural molecular conformation utilized the gradient-corrected Perdew-Burke-Ernzerhof parameterizations [67] of exchange-correlation as implemented in DMol3 [68]. A tolerance of $1x10^{-3}$ Ha was used with a smearing value of 0.005 Ha. DFT calculated energy barriers reduction in the oxidation of H_2O to H_2O_2 catalyzed using the anionic fullerene catalysts C_{44}^- to C_{136}^- are shown in Fig. 3. Results in Fig. 4 are for the water synthesis from H_2 and O_2 catalyzed using the anionic fullerene catalysts C_{44}^- to C_{136}^- as well.

Preprints (www.preprints.org) | NOT PEER-REVIEWED | Posted: 28 February 2020 doi:10.20944/preprints202002.0420.v1

Peer-reviewed version available at Int. J. Mol. Sci. 2020, 21, 3159; doi:10.3390/ijms21093159

DFT transition state calculations found the C_{52}^- and C_{60}^- anions to be numerically stable for both water oxidation and water synthesis and the C_{100}^- anion to increase the energy barrier the most in the water synthesis from H_2 and O_2. When catalyzing both water oxidation to peroxide and synthesis from H_2 and O_2, the C_{136}^- anion has proved to be the most effective in reducing the energy barrier significantly. Importantly, a single large fullerene such as the C_{136}, C_{120} or even the C_{70} could replace the Au, Pd and Sn atoms in the catalysis of H_2O_2 from H_2O in the experiments of Hutchings and collaborators [4-6] acting as a multiple-functionalized catalyst. These fullerenes have their metastable BEs close to the EAs of the used atoms in the experiments. Thus an inexpensive dynamic water purification system for the developing world could be realized [6].

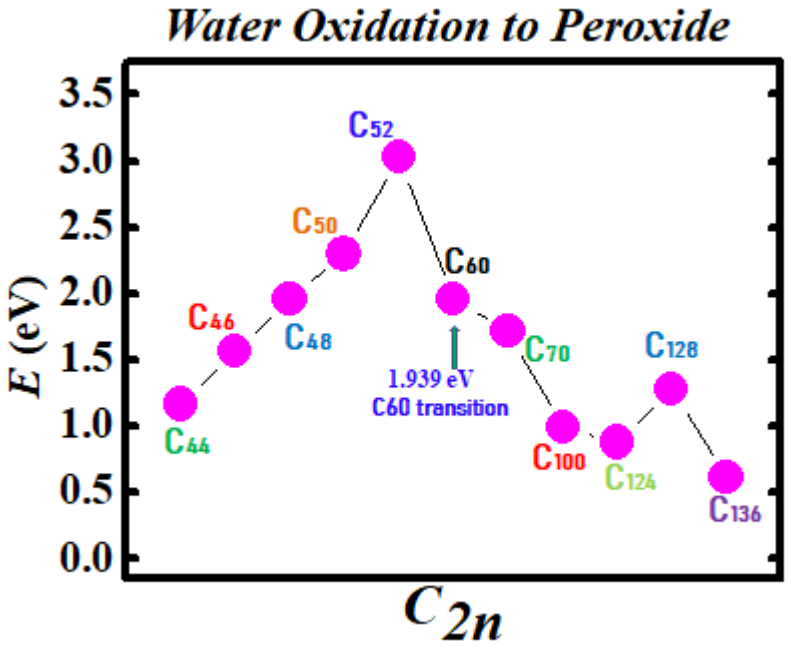

Figure 3: Transition state calculation of anionic fullerenes C_{44}^- to C_{136}^- catalyzing water oxidation to peroxide

Preprints (www.preprints.org) | NOT PEER-REVIEWED | Posted: 28 February 2020 doi:10.20944/preprints202002.0420.v1

Peer-reviewed version available at Int. J. Mol. Sci. 2020, 21, 3159; doi:10.3390/ijms21093159

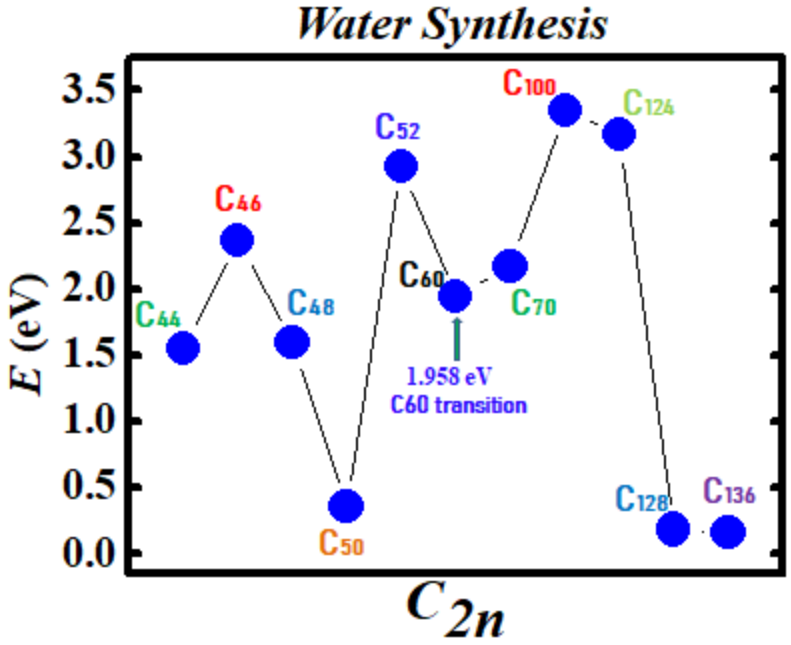

Figure 4: Transition state calculation of anionic fullerenes C_{44}^- to C_{136}^- catalyzing oxygen and hydrogen synthesis to water.

4. Summary and Conclusion

The Regge-pole calculated low-energy electron elastic TCSs for the fullerene molecules considered here are found to be characterized generally by ground, polarization-induced metastable and excited negative ion formation. The novelty and generality of the Regge-pole approach has been demonstrated through the extraction of the anionic BEs from the calculated TCSs. For ground state collisions these yield the theoretically challenging to calculate EAs and demonstrate their wide variation from fullerene to fullerene. The results here are consistent with the observation that low-energy electron-fullerene interactions are generally characterized by rich resonance structures and that the experimentally detected fullerene isomers correspond to the metastable states. They also support the conclusion that the EAs of fullerene molecules are relatively large. This should satisfy part of the requirement to increase fullerene acceptor resistance to degradation by the photo-oxidation mechanism through the use in organic solar cells of fullerenes with high EAs. The determined EAs here could also be used to construct the widely used simple model potentials for the fullerene shells, including endohedral fullerenes. Indeed, the rich resonance structures of the fullerenes TCSs and their large EAs explain the tendency of fullerenes to form compounds with electron-donor anions and their vast applications as well.

The utility of the fullerene negative ions has been demonstrated in the catalysis of water oxidation to peroxide and water synthesis from H_2 and O_2 using the anionic fullerene catalysts C_{44}^- - C_{136}^-. Transition state calculations using density functional theory found the C_{52}^- and C_{60}^- anions to be numerically stable for both water and peroxide synthesis. When catalyzing both water oxidation to peroxide and synthesis from H_2 and O_2 the C_{136}^- anion has proved to be the most effective in reducing the energy barrier significantly. Importantly, a single large fullerene such as the C_{136}, C_{120} or even the C_{60} could replace the Au, Pd and Sn atoms in the catalysis of H_2O_2 from H_2O in the experiments of Hutchings and

collaborators [4-6] acting as a multiple-functionalized catalyst. Thus an inexpensive dynamic water purification system for the developing world could be realized through the use of fullerene anions as catalysts. Furthermore, these fullerenes could also be used as catalysts in the production of methanol from methane without carbon dioxide emission with significant impact on the environment.

Table 1: Fullerene ground (GR-S), metastable (MS-n, n =1, 2, 3) and first excited (EXT-1), second excited (EXT-2) and third excited (EXT-3) anionic states binding energies (BEs). R-T refers to the energy position of the ground state R-T minimum. The measured EAs are represented as Expt. All the energies are in eV.

Full.	BEs GR-S	BEs MS-1	BEs MS-2	BEs MS-3	BEs EXT-1	BEs EXT-2	BEs EXT-3	R-T GR-S	EA Expt.
C_{44}	3.15	1.89	1.47	-	0.319	0.492	-	3.13	3.30[15]
C_{60}	2.663[19] 2.57[71] 2.23[72] 2.63[73]	1.86	1.23	-	0.203	0.378	-	2.68	2.65[10] 2.666[12] 2.683[69] 2.684[11]
C_{70}	2.70	1.77	1.27	-	0.230	0.364	0.528	2.72	2.676 [12] 2.72 [14] 2.765[13] 2.74[70]
C_{98}	3.56	2.48	1.90	-	0.294	0.350	0.442	3.54	-
C_{112}	3.31	2.53	1.73	-	0.243	0.315	0.519	3.32	-
C_{120}	3.74	2.97	2.04	1.58	0.244	0.372	0.576	3.73	-
C_{132}	3.59	2.60	1.93	1.56	0.251	0.338	0.449	3.58	-
C_{136}	3.75	2.64	2.19	1.67	0.260	0.345	0.488	3.77	-

Acknowledgment

The research was supported by the US DOE, Division of Chemical Sciences, Geosciences and Biosciences, Office of Basic Energy Sciences, Office of Energy Research. The computing facilities of the National Energy Research Scientific Computing Center are greatly appreciated.

References

1. https://pubs.rsc.org › journals › articlecollectionlanding
2. A.Z. Msezane, Z. Felfli and D. Sokolovski, J. Phys B **43**, 201001 (2010)
3. A.Z. Msezane, Z. Felfli and D. Sokolovski, Europhys News **41**, 11 (2010)
4. J.K. Edwards, A.F. Carley, A.A. Herzing, C.J. Kiely and G.J. Hutchings, J. Chem. Soc. Faraday Discuss, **138**, 225 (2008).
5. J.K. Edwards, B. Solsona, P. Landon, A.F. Carley, A. Herzing, M. Watanabe, C.J. Kiely and G.J. Hutchings, J. Mater. Chem. **15**, 4595 (2005).
6. S.J. Freakley, Q. He, J.H. Harrhy, L. Lu, D.A. Crole, D.J. Morgan, E.N. Ntainjua, J.K. Edwards, A.F. Carley, A.Y. Borisevich, C.J. Kiely and G.J. Hutchings, Science **351**, 959 (2016)
7. A. Tesfamichael, K. Suggs, Z. Felfli, X. - Q. Wang, and A.Z. Msezane, J. Phys. Chem. C, **116,** 18698 (2012)
8. A.Z. Msezane, Z. Felfli, A. Tesfamichael, K. Suggs, and X. – Q. Wang, Gold Bulletin, **3** (45), 127 (2012).
9. K. Kasdan and W.C. Lineberger, Phys. Rev. A **10**, 1658 (1974)

10. L.-S. Wang, J.J. Conceicao, C.M. Jin and R.E. Smalley, Chem. Phys. Lett. **182**, 5 (1991)
11. D.-L. Huang, P.D. Dau, H.T. Liu, and L.-S. Wang, J. Chem. Phys. **140**, 224315 (2014)
12. C. Brink, L.H. Andersen, P. Hvelplund, D. Mathur, and J.D. Voldstad, Chem. Phys. Lett. **233**, 52 (1995).
13. X.B. Wang, H.K. Woo, X. Huang, M.M. Kappes and L.S. Wang, Phys. Rev. Lett. **96**, 143002 (2006).
14. O.V. Boltalina, L.N. Sidorov, E.V. Sukhanova and E.V. Skokan, Rapid Commun. Mass Spectrom. 7, 1009 (1993).
15. H. Kietzmann, R. Rochow, G. Gantefor, W. Eberhardt, K. Vietze, G. Seifert and P.W. Fowler, Phys. Rev. Lett. **81**, 5378 (1998)
16. X.-B. Wang, H.-K. Woo, J. Yang, M.M. Kappes and L.S. Wang, J. Phys. Chem. C **111**, 7684 (2007).
17. O.V. Boltalina, I.N. Ioffe, I.D. Sorokin and L.N. Sidorov, J. Phys. Chem. A **101**, 9561 (1997).
18. A. Z. Msezane and Z. Felfli, Chem. Phys. **503**, 50 (2018)
19. Z. Felfli and A.Z. Msezane, Euro. Phys. J. D **72**, 78 (2018),
20. C. Winstead and V. McKoy, Phys. Rev. A **73**, 012711 (2006).
21. R.R. Lucchese, F.A. Gianturco and N. Sanna, Chem. Phys. Lett. **305**, 413 (1999).
22. F.A. Gianturco, R.R. Lucchese and N. Sanna, J. Phys. B **32**, 2181 (1999)
23. F.A. Gianturco and R.R. Lucchese, J. Chem. Phys. **111**, 6769 (1999).
24. A.N. Ipatov, V.K. Ivanov, J.M. Pacheco and W. Ekardt, J. Phys. B **31**, L5119 (1998).
25. V K Dolmatov, M B Cooper and M E Hunter, J. Phys. B **47**, 15002 (2014)
26. V. K. Dolmatov, M. Ya. Amusia, and L. V. Chernysheva, Phys. Rev. A **95**, 012709 (2017)
27. M.Ya. Amusia and L.V. Chernysheva, JETP Letters **101**, 503 (2015)
28. M.Ya. Amusia, L.V. Chernysheva and V.K. Dolmatov, J. Phys. B **52**, 085201 (2019)
29. M.Ya. Amusia and A.S. Baltenkov, J. Phys. B **52**, 015101 (2019)
30. H. Tanaka, L. Boesten, K. Onda and O. Ohashi, J. Phys. Soc. Jpn. **63** 485. (1994)
31. O. Elhamidi, J. Pommier and R.J. Abouaf, Int. J. Mass Spectr. **205**, 17 (2001)
32. O. Elhamidi, J. Pommier and R. Abouaf, J. Phys B **30**, 4633 (1997).
33. A. A. Viggiano, J. F. Friedman, N. S. Shuman, T. M. Miller, L. C. Schaffer and J. Troe, J. Chem. Phys. **132**, 194307 (2010)
34. V. S. Prabhudesai, D. Nandi and E. Krishnakumar, Euro Phys. J. D **35**, 261(2005)
35. A.Z. Msezane, Z. Felfli, V.R. Shaginyan and M. Ya Amusia, Int. J. Current Adv. Research **6,** 8503 (2017)
36. A.Z. Msezane and Z. Felfli, Euro Phys. J. D **72**, 178 (2018)
37. A.Z. Msezane and Z. Felfli, Applied Phys. Research **11**, 52 (2019)
38. Z. Felfli and A.Z. Msezane, J. of Atomic, Molecular, Condensate and Nano Physics **5**, 73 (2018)
39. A.Z. Msezane, J. of Atomic, Molecular, Condensate and Nano Physics **5**, 195 (2018)
40. M.V. Ryzhkov, A. L. Ivanovskii and B. Delley, Nanosystems: Physics, Chemistry, Mathematics **5,** 494 (2014)
41. M.V. Ryzhkov, A. L. Ivanovskii and B. Delley, Comp. Theor. Chem. **985,** 46 (2012)
42. M.V. Ryzhkov and B. Delley, Comp. Theor. Chem. **1013**, 70 (2013)
43. O. V. Boltalina, I. N. Ioffe, I. D. Sorokin, and L. N. Sidorov, J. Phys. Chem. **101**(50), 9561 (1997)
44. Y. Wang, R. Morales-Martínez, X. Zhang, W. Yang, Y. Wang, A. Rodríguez-Fortea, J. M. Poblet, L. Feng, S. Wang and N. Chen, J. Am. Chem. Soc. **139**, 5110 (2017)
45. P. Jin, C. Lin, Y. Li, and Y. Zhao, Int. J. Quant. Chem. **117**, e25501 (2017).
46. P. W. Dunk, N. K. Kaiser, M. Mulet-Gas, A. Rodriguez-Fortea, J. M. Poblet, H. Shinohara, C. L. Hendrickson, A. G. Marshall and H. W. Kroto, J. Am. Chem. Soc. **134**(22), 9380 (2012)
47. S. Vital, J. Marco-Martinez, S. Filippone and N. Martin, Chem. Commun. **53**, 4842 (2017).
48. A. Hiscox, B.M. Brown and M. Marletta, J. Math. Phys. **51**,102104 (2010)
49. S. C. Frautschi, Regge Poles and S-matrix Theory (New York: Benjamin, 1963) chapter X
50. V. de Alfaro and T. Regge, Potential Scattering (Amsterdam: North-Holland, 1965)
51. H. P. Mulholland, Proc. Camb. Phil. Soc. (London) **24,** 280 (1928)

52. J. H. Macek, P. S. Krstic and S. Y. Ovchinnikov, Phys. Rev. Lett. **93** 183202 (2004)
53. D. Sokolovski, Z. Felfli, S. Y. Ovchinnikov, J. H. Macek and A. Z. Msezane, Phys. Rev. A **76** 012705 (2007)
54. Z. Felfli, A. Z. Msezane and D. Sokolovski, Phys. Rev. A **79**, 012714 (2009).
55. Z. Felfli, S. Belov, N.B. Avdonina, M. Marletta, A. Z. Msezane and S.N. Naboko, in: J. Govaerts, M.N. Hounkonnou, A.Z. Msezane (Eds.), Proceedings of the Third International Workshop on Contemporary Problems in Mathematical Physics, World Scientific, Singapore, 2004, pp. 218–232.
56. S. Belov, K.-E. Thylwe, M. Marletta, A.Z. Msezane and S.N. Naboko, J. Phys. A **43**, 365301 (2010)
57. P.G. Burke and C. Tate, Comput. Phys. Commun. **1**, 97 (1969).
58. K.W. Thylwe, Eur. Phys. J. D **66**, 7 (2012)
59. M. Lezius, P. Scheier and T.D. Mark, Chem. Phys. Lett. **203**, 232 (1993)
60. T. Jaffke, E. Illenberger, M. Lezius, S. Matejcik, D. Smith and T.D. Mark, Chem. Phys. Lett. **226**, 213 (1994)
61. J. Huang, H.S. Carman and R.N. Compton, J. Phys. Chem. **99**, 1719 (1995).
62. L. Kronik, R. Fromherz, E. Ko, G. Ganteför, and J.R. Chelikowsky, Nature Mater. **1**, 49 (2002)
63. E. T. Hoke, I. T. Sachs-Quintana, M. T. Lloyd, I. Kauvar, W.R. Mateker, A. M. Nardes, C.H. Peters, N. Kopidakis and M. D. McGehee, Adv. Energy Mat. **2**, 1351 (2012)
64. W.R. Mateker and M.D. McGehee, Advanced Materials, **doi.org/10.1002/adma.201603940**
65. A. Baltenkov, S.T. Manson and A.Z. Msezane, J. Phys. B **48**, 185103 (2015)
66. W.R. Johnson and C. Guet, Phys. Rev. A **49**, 1041 (1994)
67. A. Tkatchenko and M. Scheffler, Phys. Rev. Lett. **102**, 73005 (2009)
68. DMol3 2011 Accelrys Software Inc.:San Diego, CA
69. X.B. Wang, H.K. Woo and L.S. Wang, J. Chem. Phys. 123, 051106 (2005)
70. B. Palpant, A. Otake, F. Hayakawa, Y. Negishi, G.H. Lee, A. Nakajima and K. Kaya, Phys. Rev. B **60**, 4509 (1999)
71. S. Nagase and K. Kabayashi, Chem. Phys. Lett. **228**, 106 (1999)

72. R.J. Tarento and P. Joyes, Z. Phys. D **37**, 165 (1996)
73. V.G. Zakrzewski, O. Dolgounitcheva and J.V. Ortiz, J. Phys. Chem. A **118**, 7424 (2014)